Insertion of Pyridine into an Iron−Silicon Bond and Photochemical Conversion of the Insertion Product Cp*(OC)Fe{η^3(*C,C,C*)-$C_5H_5NSiMe_2NPh_2$} to a Sandwich Compound

Masatoshi Iwata, Masaaki Okazaki,*,† and Hiromi Tobita*

Department of Chemistry, Graduate School of Science, Tohoku University, Sendai 980-8578, Japan

Received September 25, 2006

Irradiation of Cp*$(OC)_2FeSiMe_2ER_n$ (ER_n = NPh_2, NMe_2, OMe) in the presence of pyridine affords Cp*$(OC)(C_5H_5N)FeSiMe_2ER_n$, which are converted to Cp*(OC)Fe{η^3(*C,C,C*)-$C_5H_5NSiMe_2ER_n$} upon mild heating via insertion of pyridine into the iron−silicon bond. This type of pyridine insertion does not proceed in the thermal reactions of Cp*$(OC)(C_5H_5N)FeSiMe_2R$ (R = Cl, Me) and the germanium analogues, Cp*$(OC)(C_5H_5N)FeGeMe_2ER_n$ (ER_n = NPh_2, NMe_2, Me), even under more severe conditions. Treatment of Cp*$(OC)(C_5H_5N)RuMe$ with $HSiMe_2NPh_2$ at room temperature gives a 5:4 equilibrium mixture of Cp*$(OC)(C_5H_5N)RuSiMe_2NPh_2$ and Cp*(OC)HRu{κ^2(*Si,C*)-$SiMe_2N(o\text{-}C_6H_4)$(Ph)}. Heating the mixture at 100 °C does not afford an analogous insertion product, although the equilibrium is shifted to the side of the orthometalated compound. These results indicate that the insertion of pyridine is specific for the heteroatom-substituted silyliron(II) system. The insertion reaction is considered to proceed via the mechanism that involves the initial formation of an η^2(*N,C*)-pyridine complex. Migratory insertion of pyridine into the iron−silicon bond accompanied by coordination of the terminal heteroatom then results in a congested transition state, leading to the formation of an η^1-allyl intermediate, Cp*(OC)Fe-{κ^2(*C,E*)-$C_5H_5NSiMe_2ER_2$}. The formation of such a transition state is supported by kinetic analysis of the thermal conversion of Cp*$(OC)(C_5H_5N)FeSiMe_2NPh_2$ to Cp*(OC)Fe{η^3(*C,C,C*)-$C_5H_5NSiMe_2NPh_2$}, giving activation parameters of $\Delta H^{\ddagger} = 93(2)$ kJ mol^{-1}, $\Delta S^{\ddagger} = -53(6)$ J mol^{-1} K^{-1}, and $\Delta G^{\ddagger}_{298\ K} = 109(3)$ kJ mol^{-1}. The η^3-allyl complex is finally formed through dissociation of the amino part. Irradiation of Cp*(OC)Fe{η^3(*C,C,C*)-$C_5H_5NSiMe_2NPh_2$} causes dissociation of a carbonyl ligand to produce a new type of sandwich compound, Cp*Fe(η^5-$C_5H_5NSiMe_2NPh_2$).

Introduction

The hydrosilylation of unsaturated organic compounds is one of the most important reactions in organosilicon chemistry and has been examined thoroughly and extensively for application in the industrial production of organosilicon compounds. In research laboratories, hydrosilylation of unsaturated organic compounds provides not only synthetic intermediates in organic syntheses but also silicon-based new materials.[1] However, the scope of the hydrosilylation of aromatic compounds is extremely narrow. Pyridine is the only example of an aromatic substrate that has been successfully hydrosilylated. Heterogeneous catalytic hydrosilylation of pyridines was achieved by Cook and Lyons many years ago.[2] In 1998, Harrod et al. reported for the first time the homogeneously catalyzed hydrosilylation of pyridines, mixing $PhMeSiH_2$ and pyridine in the presence of Cp_2TiMe_2 to produce *N*-silyl-2,3,4-trihydropyridine accompanied by the formation of $(PhMeHSi)_n$.[3]

In the modified Chalk−Harrod mechanism, first proposed by Seitz and Wrighton, the insertion of an alkene molecule into a metal−silicon bond is a crucial step in the catalytic hydrosilylation of alkene.[4,5] The reactions of various isolated transition-metal silyl complexes with unsaturated organic molecules have thus been investigated in an attempt to gain insight into this catalytic hydrosilylation mechanism.[6] Although there are numerous examples of the insertion of alkenes, alkynes, nitriles, and carbonyl compounds into metal−silicon bonds, little is known regarding the insertion of aromatic compounds into these bonds. Research on this type of stoichiometric reaction could stimulate the development of the little-explored transition-metal-catalyzed hydrosilylation of aromatic compounds. Woo and Tilley observed the insertion of pyridine into the zirconium−silicon bond in the reaction of CpCp*Zr[$Si(SiMe_3)_3$]Me and pyridine to afford CpCp*Zr[κ^1(*N*)-$NC_5H_5Si(SiMe_3)_3$]Me, in which the regiospecificity is different from the intermediate in the Cp_2TiMe_2-catalyzed hydrosilylation of pyridine.[7] We herein report the insertion of pyridine into an iron−silicon bond by the thermal

* To whom correspondence should be addressed. E-mail: mokazaki@scl.kyoto-u.ac.jp (M.O.); tobita@mail.tains.tohoku.ac.jp (H.T.).

† Present address: International Research Center for Elements Science (IRCELS), Institute for Chemical Research, Kyoto University.

(1) Ojima, I.; Li, Z.; Zhu, J. In *The Chemistry of Organic Silicon Compounds*; Rappoport, Z., Apeloig, Y., Eds.; Wiley: New York, 1998; Vol. 2, Chapter 35, pp 1687−1792.

(2) Cook, N. C.; Lyons, J. E. *J. Am. Chem. Soc.* **1966**, *88*, 3396−3403.

(3) (a) Hao, L.; Harrod, J. F.: Lebuis, A.-M.; Mu, Y.; Shu, R.; Samuel, E.; Woo, H.-G. *Angew. Chem. Int. Ed.* **1998**, *37*, 3126−3129. (b) Harrod, J. F.; Shu, R.; Woo, H.-G.; Samuel, E. *Can. J. Chem.* **2001**, *79*, 1075−1085.

(4) (a) Schroeder, M. A.; Wrighton, M. S. *J. Organomet. Chem.* **1977**, *128*, 345−358. (b) Reichel, C. L.; Wrighton, M. S. *Inorg. Chem.* **1980**, *19*, 3858−3860. (c) Randolph, C. L.; Wrighton, M. S. *J. Am. Chem. Soc.* **1986**, *108*, 3366−3374. (d) Seitz, F.; Wrighton, M. S. *Angew. Chem., Int. Ed. Engl.* **1988**, *27*, 289−291.

(5) Sakaki, S.; Sumimoto, M.; Fukuhara, M.; Sugimoto, M.; Fujimoto, H.; Matsuzaki, S. *Organometallics* **2002**, *21*, 3788−3802.

(6) (a) Eisen, M. S. In *The Chemistry of Organic Silicon Compounds*; Rappoport Z., Apeloig, Y., Eds.; Wiley: New York, 1998; Vol. 2, Chapter 35, pp 2037−2128. (b) Tilley, T. D. In *The Silicon-Heteroatom Bond*; Patai, S., Rappoport, Z., Eds.; Wiley: New York, 1991; Chapters 9, 10, pp 245−308, pp 309−364. (c) Braunstein, P.; Knorr, M. *J. Organomet. Chem.* **1995**, *500*, 21−38.

(7) Woo, H.-G.; Tilley, T. D. *J. Organomet. Chem.* **1990**, *393*, C6−C9.

10.1021/om060873n CCC: $33.50
Publication on Web 11/17/2006

reaction of Cp*(OC)(C_5H_5N)$FeSiMe_2NPh_2$ to give Cp*(OC)-Fe{η^3(*C*,*C*,*C*)-$C_5H_5NSiMe_2NPh_2$}. In this product, the silicon atom is bound to the pyridine nitrogen atom, while the iron atom is bound to the carbon atom. The product thus corresponds to the proposed intermediate in the catalytic reaction. To elucidate the essential requirements for the insertion step, thermal reactions of Cp*(OC)(C_5H_5N)$FeER_3$ (ER_3 = $SiMe_2$-NMe_2, $SiMe_2Cl$, $SiMe_3$, $SiMe_2OMe$, $GeMe_2NPh_2$, $GeMe_2NMe_2$, and $GeMe_3$) and selected ruthenium analogues are examined. Irradiation of the insertion product affords an unprecedented sandwich compound, Cp*Fe(η^5-$C_5H_5NSiMe_2NPh_2$), which is unequivocally determined by X-ray diffraction study. Some of the results reported here have appeared elsewhere in a preliminary form.[8]

Results and Discussion

The synthesis of the aminosilyliron(II) complexes Cp*-$(OC)_2FeSiMe_2NR_2$ (R = Ph (**1a**) and Me (**1b**)) by irradiation of Cp*$(OC)_2FeMe$ and $HSiMe_2NPh_2$ or treatment of Li[Cp*-$(OC)_2Fe$] with $ClSiMe_2NMe_2$ in diethyl ether was presented in a previous paper.[9] Ultraviolet (UV) irradiation of **1a** in the presence of pyridine in toluene caused the solution to turn from yellow to dark red in color (eq 1). Removal of volatiles followed by recrystallization of the residue from toluene/hexane solution at −30 °C gave dark red crystals of Cp*(OC)(C_5H_5N)$FeSiMe_2$-NPh_2 (**2a**) in 72% yield. The NMe_2 analogue Cp*(OC)-(C_5H_5N)$FeSiMe_2NMe_2$ (**2b**) was synthesized similarly in 61% yield by photoreaction between Cp*$(OC)_2FeSiMe_2NMe_2$ (**1b**) and pyridine. All spectroscopic data are in good agreement with the structures of **2**. The $^{29}Si\{^1H\}$ nuclear magnetic resonance (NMR) signals of **2** were observed at δ 53.5 (**2a**) and 56.9 (**2b**). Substitution of CO by the electron-releasing pyridine ligand caused a significant shift of ν_{CO} to lower energies (**1a**, 1973, 1917 cm^{-1}; **1b**, 1971, 1911 cm^{-1}; **2a**, 1878 cm^{-1}; **2b**, 1869 cm^{-1}).

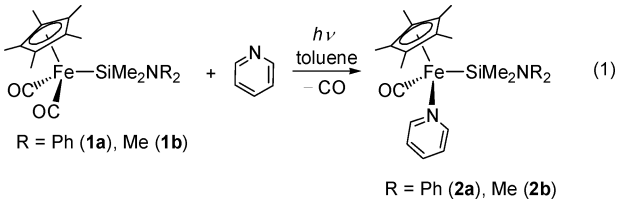

The molecular structure of **2a** is depicted in Figure 1. Complex **2a** takes a typical three-legged piano-stool geometry in which one carbonyl ligand in **1a** is replaced with pyridine. The Fe−Si bond distance (2.3330(4) Å) for **2a** is shorter than that in **1a** (2.3355(7) Å), while the Si−N1 bond distance (1.799-(1) Å) is longer than that in **1a** (1.787(2) Å).[9] These structural features are attributable to the electron-rich iron center upon coordination of the electron-releasing pyridine ligand, which enhances back-donation from the iron dπ orbital to the Si−N σ^* orbital.[10] The electron-richness is also reflected in the elongation of the O−C15 bond (1.168(2) Å) compared to those in **1a** (1.159(3), 1.151(4) Å).

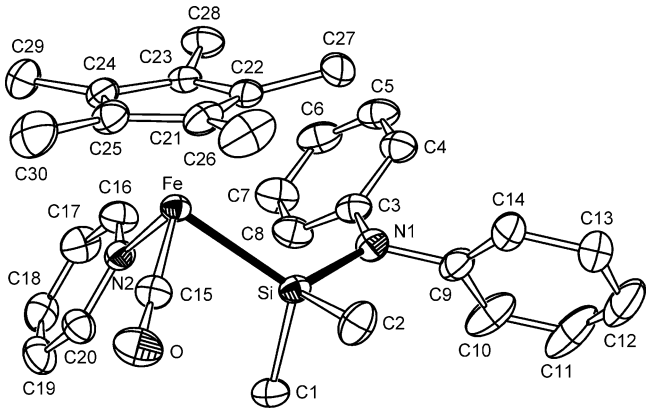

Figure 1. ORTEP drawing of **2a** with thermal ellipsoids at the 50% probability level. Selected bond distances (Å) and angles (deg): Fe−Si 2.3330(4), Fe−N2 1.991(1), Fe−C15 1.716(2), Si−N1 1.799(1), O−C15 1.168(2), Si−Fe−N2 92.84(4), Si−Fe−C15 80.97(5), N2−Fe−C15 97.20 (6), Fe−Si−N1 118.70(5).

Complex **2a** can be regarded as a key intermediate in the transition-metal-catalyzed hydrosilylation of pyridine. If the reaction is operative, the pyridine N−C unsaturated bond would be inserted into the Fe−Si bond. The feasibility of this reaction was examined by carrying out the thermal reaction of **2a** as follows. A toluene solution of **2a** was heated at 60 °C for 2 days (eq 2), after which volatiles were removed in vacuo and the residue was extracted with pentane. Recrystallization of the concentrated pentane extract at −30 °C gave orange crystals of Cp*(OC)Fe{η^3(*C*,*C*,*C*)-$C_5H_5NSiMe_2NPh_2$} (**3a**) in 55% yield. The thermal reaction of **2b** was performed under the same conditions to afford Cp*(OC)Fe{η^3(*C*,*C*,*C*)-$C_5H_5NSiMe_2NMe_2$} (**3b**) in 86% NMR yield. However, **3b** was an air-sensitive oil and isolation was not successful. Characterization of **3b** was performed by comparison with the NMR spectra of **3a** (vide infra).

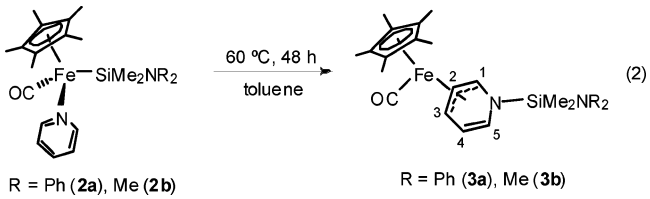

The structure of **3a** was unequivocally determined by the X-ray diffraction study. An ORTEP drawing of **3a** is shown in Figure 2. The complex has one Cp* and one CO ligand, and an η^3-allyl fragment formed through the insertion of pyridine into the iron−silicon bond, in which the aminosilyl group is bound to the nitrogen atom of pyridine. The geometry of complex **3** is thus the same as that suggested for the intermediate in the catalytic hydrosilylation of pyridine by Cp_2TiMe_2.[3] The distances of the Si−N1 and Si−N2 bonds are 1.747(2) and 1.742-(2) Å, respectively, falling within the normal range for single silicon−nitrogen bonds. The bonding parameters are also in the range expected for the η^3-allyl iron complexes:[11] the carbon−carbon bond distances in the allylic moiety are 1.413(4) Å (C15−C16) and 1.412(4) Å (C16−C17). The distances between iron and allylic carbon atoms are 2.134(3) Å (Fe−C15), 1.995-(3) Å (Fe−C16), and 2.141(3) Å (Fe−C17), and the bond lengths of C17−C18 and C18−C19 are 1.471(4) and 1.332(4) Å, respectively, which corresponds to the values for the single

(8) Iwata, M.; Okazaki, M.; Tobita, H. *Chem. Commun.* **2003**, 2744−2745.

(9) Okazaki, M.; Iwata, M.; Tobita, H.; Ogino, H. *Dalton Trans.* **2003**, 1114−1120.

(10) (a) Schilling, B. E. R.; Hoffmann, R.; Lichtenberger, D. L. *J. Am. Chem. Soc.* **1979**, *101*, 585−591. (b) Lichtenberger, D. L.; Rai-Chaudhuri, A. *J. Am. Chem. Soc.* **1991**, *113*, 2923−2930. (c) Hübler, K.; Hunt, P. A.; M. Maddock, S.; Rickard, C. E. F.; Roper, W. R.; Salter, D. M.; Schwerdtfeger, P.; Wright, L. J. *Organometallics* **1997**, *16*, 5076−5083.

(11) Orpen, A. G.; Brammer, L.; Allen, F. H.; Kennard, O.; Watson, D. G.; Taylor, R. *J. Chem. Soc., Dalton Trans.* **1989**, S1−S83.

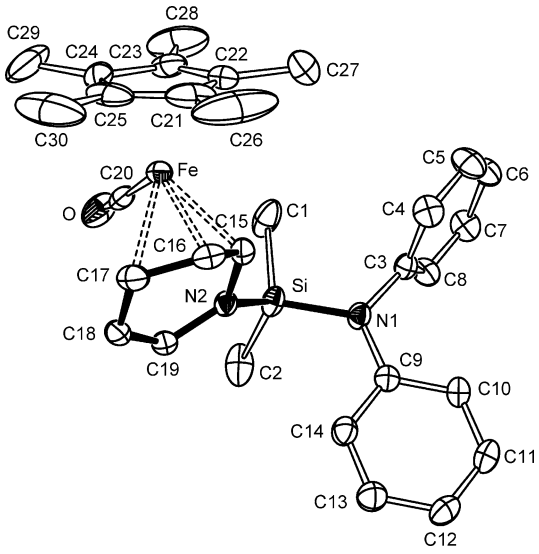

Figure 2. ORTEP drawing of **3a** with thermal ellipsoids at the 50% probability level. Selected bond distances (Å) and angles (deg): Fe−C15 2.134(3), Fe−C16 1.995(3), Fe−C17 2.141(3), Fe−C20 1.730(3), C20−O 1.161(4), Si−N1 1.747(2), Si−N2 1.742(2), N2−C15 1.442(3), N2−C19 1.390(3), C15−C16 1.413(4), C16−C17 1.412(4), C17−C18 1.471(4), C18−C19 1.332(4), Si−N2−C15 118.0(2), Si−N2−C19 125.0(2), C15−N2−C19 116.3(2).

and double bond. The structurally related molybdenum complexes with an η^3-allyl ligand have been synthesized by Malinakova and Liebeskind by a very different approach.[12]

The structures of **3** are also supported by the spectroscopic data in solution. The ^{1}H and ^{13}C NMR signals of the inserted pyridine moiety for **3a** were observed at δ (^{1}H) 1.77 (2), 3.74 (3), 5.30 (4), 5.47 (5), and 5.73 (1) and δ (^{13}C) 45.1 (2), 51.2 (3), 76.9 (1), 110.8 (4), and 121.1 (5), respectively, where values in parentheses denote the positions of the atoms (eq 2). Assignments were established on the basis of two-dimensional ^{1}H−^{1}H and ^{13}C−^{1}H COSY spectral data. The chemical shifts are consistent with the η^3-allyl-type coordination of the $C_5H_5N(SiMe_2NPh_2)$ fragment. Both the X-ray and NMR data thus clearly indicate that the aromaticity of the pyridine moiety of **3** is disrupted. The ^{29}Si NMR signal at δ −2.3 for **3a** is shifted toward the high-field region compared with that in **2a** (δ 53.5), supporting migration of the aminosilyl ligand from the iron center to the nitrogen atom. The CO vibration of **3a** (1911 cm^{-1}) now appears in the higher energy region compared to that of the starting material **2a** (1878 cm^{-1}), supporting the replacement of silyl and pyridine ligands with an η^3-allyl ligand.

Thermal reactions were also attempted for selected silyl(pyridine)iron complexes of the type $Cp^*(OC)(C_5H_5N)FeSiMe_2R$ (R = Cl (**2c**), Me (**2d**), and OMe (**2e**)) (Scheme 1). Under the same conditions as described by eq 2, however, no reaction took place. Thermolysis of **2c** and **2d** under more forced conditions resulted in decomposition of the complexes. Reaction of **2e** at 90 °C for 24 h gave the pyridine-inserted product $Cp^*(OC)Fe\{\eta^3(C,C,C)\text{-}C_5H_5NSiMe_2OMe\}$ (**3e**) in 18% NMR yield together with $Me_2Si(OMe)_2$ (24%), unidentified products, and recovered **2e** (9%). Purification of **3e** has yet to be achieved. Complex **3e** was characterized by comparison with the NMR data of **3a** and **3b**. The ^{1}H and ^{13}C NMR signals of the inserted pyridine moiety in **3e** were observed at δ (^{1}H) 1.79 (2), 3.70 (3), 5.21 (4), 5.32 (5), and 5.62 (1) and δ (^{13}C) 45.5 (2), 51.0 (3), 77.9 (1), 110.3 (4), and 121.5 (5), respectively. The ^{29}Si NMR signal was observed at δ 2.2. These NMR spectroscopic features are quite similar to those for **3a** and **3b**. The reactivity of **2a**−**e** toward the insertion of pyridine decreased in the order **2a**, **2b** (reacted quantitatively) > **2e** (reacted slowly and in low yield) > **2c**, **2d** (no reaction).

To elucidate the critical factor driving the migratory insertion of pyridine, the thermal reactions of germyl(pyridine) complexes were also examined. Germyl complexes of the type $Cp^*(OC)_2FeGeMe_2R$ (R = NPh_2 (**1f**), NMe_2 (**1g**), Me (**1h**)) were synthesized by reaction of $K[Cp^*(OC)_2Fe]$ with the corresponding germanium halides (Scheme 2). Substitution of one carbonyl ligand with pyridine to give $Cp^*(OC)(C_5H_5N)FeGeMe_2R$ (R = NPh_2 (**2f**), NMe_2 (**2g**), Me (**2h**)) was achieved by UV irradiation of the complexes in the presence of pyridine. Thermal conversion of **2f**−**h** to the η^3-allyl complexes, $Cp^*(OC)Fe\{\eta^3(C,C,C)\text{-}C_5H_5NGeMe_2R\}$, did not take place at 60 °C. Under more forced conditions of 110 °C, **2f**−**h** decomposed to yield several unidentified products.

Kinetic study of the thermal conversion from **2a** to **3a** in benzene-d_6 was conducted over the temperature range 328−348 K to obtain plots of $\ln(A_t/A_0)$ (A = [**2a**]) with respect to time t and the first-order rate constants. An Eyring plot gives activation parameters of $\Delta H^{\ddagger} = 93(2)$ kJ mol^{-1}, $\Delta S^{\ddagger} = -53(6)$ J mol^{-1} K^{-1}, and $\Delta G^{\ddagger}_{298\ K} = 109(3)$ kJ mol^{-1} (see Supporting Information). The relatively large negative $\Delta S^{\ddagger}$ value indicates the existence of a sterically more congested transition state than **2a**.

A plausible formation mechanism for **3** involving initial formation of an $\eta^2(N,C)$-pyridine complex **A** is illustrated in Scheme 3. The migratory insertion of pyridine into the iron−silicon bond, accompanied by coordination of the terminal amino group, results in the transition state **B**, leading to the formation of an η^1-allyl amino-coordinated complex **C**. Finally, **C** isomerizes to the η^3-allyl complex **3** through dissociation of the amino part.

In **2**, the coordination of electron-releasing Cp*, pyridine, and aminosilyl ligands results in an extremely electron-rich iron center. This type of an electronic factor may facilitate isomerization of **2** to an $\kappa^2(N,C)$-pyridine complex (i.e., **A**). The electron density of the iron center is roughly estimated from the wave number of ν_{CO} to decrease in the order **2b** (1869 cm^{-1}) > **2d**, **2e** (1873 cm^{-1}) > **2h** (1876 cm^{-1}) > **2g** (1877 cm^{-1}) > **2a** (1878 cm^{-1}) > **2c** (1882 cm^{-1}) > **2f** (1888 cm^{-1}). As the tendency for insertion of pyridine into the iron−silicon or iron−germanium bond does not correlate with the electron-richness of the iron center, transformation of **2** to **A** does not appear to be a rate-determining step. On the other hand, the existence of an amino or methoxy group capable of coordination to the coordinatively unsaturated iron center appears to be crucial, lowering the activation barrier for the insertion of pyridine into the iron−silicon bond. Coordination of the Si−OR[13] or Si−NR_2[14] group to metals has been well documented. This scenario is supported by the kinetic study, which suggested a large negative value of $\Delta S^{\ddagger}$ consistent with the transient generation of the sterically congested form **B**.

(12) (a) Malinakova, H. C.; Liebeskind, L. S. *Org. Lett.* **2000**, *2*, 3909−3911. (b) Malinakova, H. C.; Liebeskind, L. S. *Org. Lett.* **2000**, *2*, 4083−4086. (c) Zhang, Y.; Liebeskind, L. S. *J. Am. Chem. Soc.* **2006**, *128*, 465−472.

(13) (a) Atagi, L. M.; Mayer, J. M. *Organometallics* **1994**, *13*, 4794−4803. (b) Klei, S. R.; Tilley, T. D.; Bergman, R. G. *Organometallics* **2002**, *21*, 4648−4661. (c) Sakaba, H.; Watanabe, S.; Kabuto, C.; Kabuto, K. *J. Am. Chem. Soc.* **2003**, *125*, 2842−2843.

(14) (a) Aslanidis, P.; Grobe, J. *J. Organomet. Chem.* **1983**, *249*, 103−126. (b) Schwarz, M.; Kickelbick, G.; Schubert, U. *Eur. J. Inorg. Chem.* **2000**, 1811−1817. (c) Döhring, A.; Göhre, J.; Jolly, P. W.; Kryger, B.; Rust, J.; Verhovnik, G. P. J. *Organometallics* **2000**, *19*, 388−402.

Scheme 1

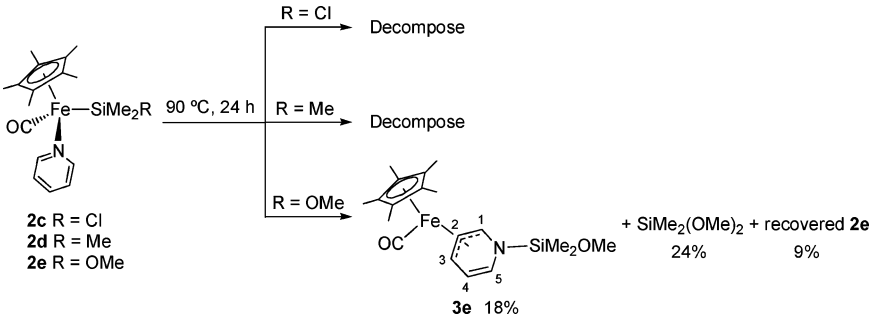

Scheme 2

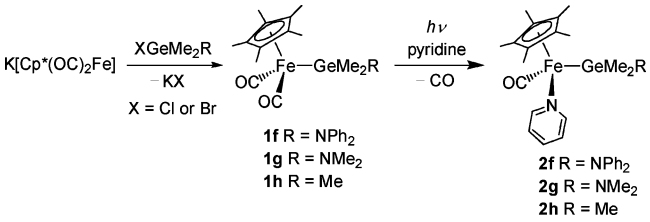

Scheme 3

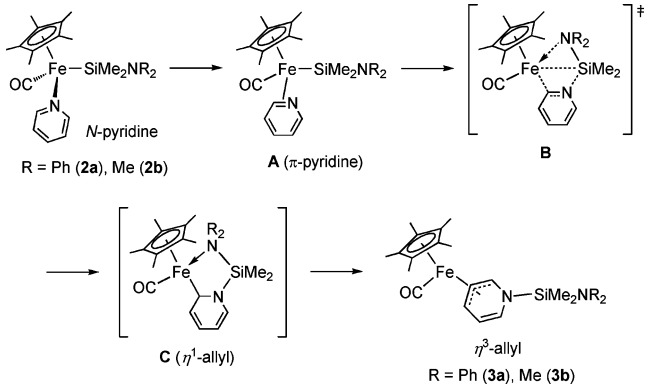

Insertion of the nitrile nitrogen−carbon triple bond into the metal−silicon bonds has been reported by Bergman and Brookhart,[15] Tilley,[13b] Nakazawa,[16] and our group.[17] The cationic complex $[Cp^*(Me_3P)(CH_2Cl_2)Rh(SiPh_3)]^+$ activates the carbon−carbon bonds of aryl and alkyl cyanides RCN to give $[Cp^*(Me_3P)Rh(R)(CNSiPh_3)]^+$, the η^2-iminoacyl intermediate $[Cp^*(Me_3P)Rh(\eta^2(N,C)\text{-}RC{=}N(SiPh_3))]^+$ of which has been isolated and characterized by X-ray diffraction study. Tilley et al. also observed similar activation of nitriles by a cationic iridium(III) silyl complex. Nakazawa et al. reported the insertion of acetonitrile into an iron−silicon bond. Photoreaction of $Cp(OC)_2FeSiMe_3$ in acetonitrile solution containing $P[MeN(CH_2)_2NMe](OMe)$ resulted in cleavage of the acetonitrile carbon−carbon bond to give $Cp(OC)LFeMe$, CpL_2FeMe, and $CpL_2Fe(CN)$ ($L = P[MeN(CH_2)_2NMe](OMe)$). The same reaction was also attempted for the germyl analogue $Cp(OC)_2FeGeMe_3$. However, irradiation under the same conditions gave the substitution product $Cp(OC)LFeGeMe_3$. The silyl ligand on the iron is thus indispensable for the insertion of acetonitrile followed by carbon−carbon bond cleavage, in good agreement with the present results.

The possibility of pyridine insertion into the ruthenium−silicon bond by the same approach was also investigated. Treatment of $Cp^*(OC)(C_5H_5N)RuMe$ with $HSiMe_2NPh_2$ at room temperature gave a mixture of $Cp^*(OC)(C_5H_5N)RuSiMe_2NPh_2$ (**2i**) and $Cp^*(OC)HRu\{\kappa^2(Si,C)\text{-}SiMe_2N(o\text{-}C_6H_4)(Ph)\}$ (**4i**) in a 5:4 molar ratio. Recrystallization from toluene/pentane at −30 °C afforded a mixture of **2i** (29%) and **4i** (31%) as orange and light yellow crystals, respectively. The two crystal types were successfully separated on the basis of color. To avoid formation of the orthometalated **4i**, the reaction of $Cp^*(OC)(C_5H_5N)RuMe$ with $HSiMe_2NPh_2$ was carried out in the presence of excess pyridine, requiring more severe conditions than those suggested in eq 3 in order to dissociate the pyridine ligand. The reaction gave **2i** as a sole product in 72% yield (eq 4). The NEt_2 analogue **2k** was synthesized in the same manner in 38% yield.

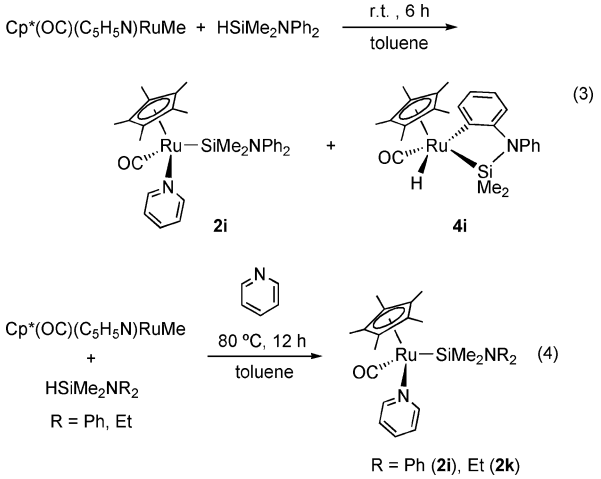

In complex **2i**, two methyl groups on silicon are diastereotopic and the NMR signals were observed inequivalently at δ (^{1}H) 0.47 and 0.61 and δ (^{13}C) 6.6 and 8.4. The ^{1}H and ^{13}C NMR signals for the coordinated pyridine are reasonably assigned as described in the Experimental Section. The ^{29}Si{^{1}H} NMR spectrum exhibits a signal at δ 37.8, which is typical of silylruthenium complexes. The infrared (IR) spectrum displays a strong band at 1890 cm^{-1} assignable to the CO stretching band. In the ^{1}H NMR spectrum of **4i**, the resonance of the Ru−H fragment appeared in the normal region as a very broad signal. At 253 K, this signal became a sharp singlet (δ −10.53). The observed fluxional behavior may be attributable to a combined Berry−Turnstile isomerization as proposed by Smith and Coville[18] or to a reversible E−H reductive elimination/oxidative addition process (E = C or Si). No direct evidence is available on which to distinguish between these two putative processes.

(15) (a) Taw, F. L.; White, P. S.; Bergman, R. G.; Brookhart, M. *J. Am. Chem. Soc.* **2002**, *124*, 4192−4193. (b) Taw, F. L.; Mueller, A. H.; Bergman, R. G.; Brookhart, M. *J. Am. Chem. Soc.* **2003**, *125*, 9808−9813.

(16) Nakazawa, H.; Kawasaki, T.; Miyoshi, K.; Suresh, C. H.; Koga, N. *Organometallics* **2004**, *23*, 117−126.

(17) Hashimoto, H.; Matsuda, A.; Tobita, H. *Organometallics* **2006**, *25*, 472−476.

(18) Smith, J. M.; Coville, N. J. *Organometallics* **1996**, *15*, 3388−3392.

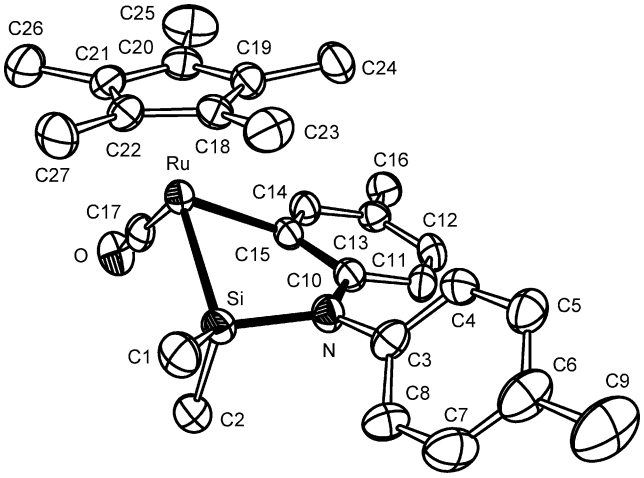

Figure 3. ORTEP drawing of **4j** with thermal ellipsoids at the 50% probability level. Selected bond distances (Å) and angles (deg): Ru−Si 2.4353(17), Ru−C15 2.144(6), Ru−C17 1.854(6), Si−N 1.781(5), C15−Ru−Si 72.18(15), C17−Ru−Si 100.8(2), C17−Ru−C15 83.7(2).

The ^{29}Si{^{1}H} NMR spectrum at 298 K exhibits a singlet at δ 52.2. In the IR spectrum, the formation of an Ru(IV) center through orthometalation is reflected in the large shift of ν_{CO} to a higher energy region (**2i**, 1890 cm^{-1}; **4i**, 1973 cm^{-1}) due to a decrease in π-back-donation from the Ru dπ orbital to the CO π^* orbital.

As the crystals of **4i** were not suitable for X-ray diffraction study, the *p*-tolyl analogue, Cp*(OC)HRu{κ^2(*Si*,*C*)-SiMe$_2$N(*o*-C$_6$H$_3$(4-Me))(*p*-Tol)} (**4j**), was synthesized in a similar manner. The molecular structure of **4j** is illustrated in Figure 3. The ruthenium(IV) center of **4j** includes Cp* and CO ligands and a five-membered ring consisting of Ru, Si, N, C10, and C15 atoms formed through C−H activation at the *o*-position of the *p*-Tol group. The bite angle of C15−Ru−Si is 72.18(15)°, and the Ru−Si and Ru−C15 bond distances are 2.4353(17) and 2.144-(6) Å, respectively, within the range expected for each single bond. The hydrogen atom connected to the ruthenium center could not be located crystallographically but most probably exists inside the widened Si−Ru−C17 angle (100.8(2)°), as supported by the ^{1}H NMR spectroscopic data. A similar five-membered silaosmacycle has been reported by Tilley et al.,[19] who reacted the osmium alkyl complex Cp*(Me$_3$P)$_2$OsCH$_2$-SiMe$_3$ with HSiMe$_2$S(*p*-Tol) in cyclohexane at 115 °C to give Cp*(Me$_3$P)(H)Os{κ^2(*Si*,*C*)-SiMe$_2$S(*o*-C$_6$H$_3$(4-Me))} and Cp*-(Me$_3$P)$_2$OsS(*p*-Tol) in an 8:1 molar ratio. The same authors also described the thermal reaction of the ruthenium analogue, Cp*-(Me$_3$P)$_2$RuCH$_2$SiMe$_3$, with HSiMe$_2$S(*p*-Tol) in toluene at 100 °C to give Cp*(Me$_3$P)$_2$RuSiMe$_2$S(*p*-Tol) exclusively, without formation of the orthometalated product.[20]

When crystals of **2i** were dissolved in benzene-d_6, **2i** was gradually converted to **4i** accompanied by the release of pyridine. Equilibrium was reached at a 1:1 molar ratio ([**2i**] = [**4i**] = 13 mM) within several hours at 25 °C (eq 5). Heating of the equilibrium mixture at 100 °C for 48 h did not promote insertion, but the equilibrium was shifted to the right side to yield a mixture of **2i** and **4i** in a 2:9 molar ratio. Monitoring the thermal reaction of **2k** by ^{1}H NMR spectroscopy revealed no changes at 60 °C but the emergence of a series of weak

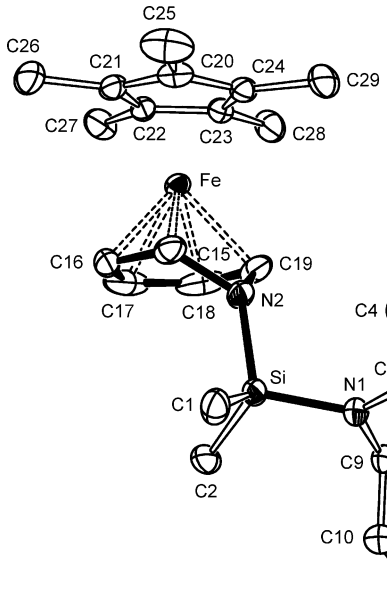

Figure 4. ORTEP drawing of **5a** with thermal ellipsoids at the 50% probability level. Selected bond distances (Å) and angles (deg): Fe−C15 2.044(2), Fe−C16 2.014(2), Fe−C17 2.024(2), Fe−C18 2.003(2), Fe−C19 2.037(2), C15−C16 1.416(3), C16−C17 1.399(4), C17−C18 1.404(4), C18−C19 1.408(3), N2−C15 1.442-(2), N2−C19 1.442(2), Si−N1 1.751(1), Si−N2 1.736(1), C15−C16−C17 116.7(2), C16−C17−C18 118.0(2), C17−C18−C19 116.9(2), N2−C15−C16 118.1(2), N2−C19−C18 118.2(2), C15−N2−C19 99.4(1), Si−N2−C15 124.2(1), Si−N2−C19 121.6(1).

signals after heating at 80 °C for 4 h. However, signals characteristic of the pyridine-insertion product were not detected at any time, indicating that the insertion of pyridine into the metal−silicon bonds is peculiar to the iron−silicon system. This is likely due to the lower bond dissociation energy for the iron−silicon bond.

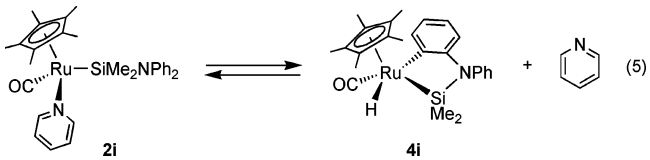

UV irradiation of **3a** led to the dissociation of a carbonyl ligand, affording a new entry of sandwich compound Cp*Fe-(η^5-C$_5$H$_5$NSiMe$_2$NPh$_2$) (**5a**) in 71% yield (eq 6). The elemental analysis and mass spectral data for **5a** are consistent with this formula. The IR spectrum did not display strong bands in the terminal CO region, strongly supporting the absence of a carbonyl ligand in **5a**. The ^{1}H and ^{13}C NMR signals of the inserted pyridine fragment appeared at δ (^{1}H) 2.67 (1), 3.36 (2), and 5.48 (3) and δ (^{13}C) 45.2 (1), 78.5 (2), and 85.0 (3), respectively (numbers in parentheses denote the positions, see eq 6). The ^{29}Si NMR signal was observed at δ −14.2, which is typical of the tetravalent silicon atom bonded to the nitrogen atom.

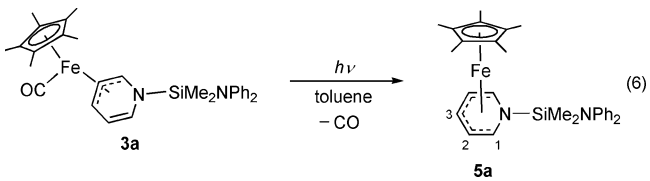

The molecular structure of **5a** is shown in Figure 4. The five carbon atoms of the η^5-azacyclohexadienyl ligand (C15−C19)

(19) Wanandi, P. W.; Tilley, T. D. *Organometallics* **1997**, *16*, 4299−4313.

(20) Grumbine, S. K.; Straus, D. A.; Tilley, T. D.; Rheingold, A. L. *Polyhedron* **1995**, *14*, 127−148.

are nearly coplanar with a mean deviation of 0.0130 Å from planarity. The dihedral angle between two least-square planes defined by C15−C16−C17−C18−C19 (plane 1) and by C20−C21−C22−C23−C24 (plane 2) is 3.8°. The nitrogen atom is located at a distance of 0.724 Å from plane 1. The bond distances of C15−C16 (1.416(3) Å), C16−C17 (1.399(4) Å), C17−C18 (1.404(4) Å), and C18−C19 (1.408(3) Å) are the intermediates between carbon−carbon single and double bonds, whereas the bond distances of N2−C15 (1.442(2) Å) and N2−C19 (1.442(2) Å) are in the normal range for nitrogen−carbon single bonds, indicating delocalization throughout the five carbon atoms inside the six-membered ring. Thus, **5a** can be best described as a sandwich compound, in which the iron(II) center is intercalated between the Cp* and η^5-$C_5H_5NSiMe_2$-NPh_2 π-conjugated ligands. The half-sandwich manganese complex with the η^5-azacyclohexadienyl ligand has previously been reported by Homrighausen,[21] who synthesized the manganese complex by coupling of an isocyanide ligand with two alkyne molecules on the manganese.

Conclusion

The structure of **3a** formed through the insertion of a heterocyclic aromatic compound (pyridine) into the metal−silicon bond was characterized by X-ray diffraction study for the first time. In complex **3a**, the silicon atom is bound to the pyridine nitrogen atom, while the iron atom is bound to carbon atoms, corresponding to the catalytic intermediate proposed by Harrod et al.[3] Among the $Cp^*(OC)(C_5H_5N)MER_3$ systems examined (i.e., M = Fe, E = Si, Ge and M = Ru, E = Si), the insertion of pyridine proceeded exclusively in the case of aminosilyliron complexes under the moderate conditions. The amino group is considered to stabilize the transition state and/or the intermediate, allowing the insertion reaction to proceed upon coordination to the coordinatively unsaturated iron center. This finding provides valuable insight into the catalytic mechanism for hydrosilylation of heterocyclic aromatic compounds. It should be noted that the introduction of an amino group onto silicon also has potential advantages with respect to further functionalization of the product, as the amino group can be readily replaced with nucleophiles.

Photolysis of **3a** with an η^3-$C_5H_5NSiMe_2NPh_2$ ligand resulted in rearrangement to give **5a** with an η^5-$C_5H_5NSiMe_2NPh_2$ through dissociation of one carbonyl ligand. Complex **5a** represents a new type of metallocene having two π-conjugated ligands, Cp* and η^5-$C_5H_5NSiMe_2NPh_2$.

Experimental Section

General Procedures. All manipulations were carried out under a dry nitrogen atmosphere. Reagent-grade toluene, hexane, pentane, and diethyl ether were distilled from sodium-benzophenone ketyl immediately prior to use. Benzene-d_6 was dried over a potassium mirror and transferred into an NMR tube under vacuum. Pyridine was distilled from KOH prior to use. $Cp^*(OC)_2FeSiMe_2NR_2$ (R = Ph (**1a**) and Me (**1b**)),[9] $Cp^*(OC)(C_5H_5N)FeMe$,[22] $Cp^*(OC)_2$-$FeSiMe_2Cl$ (**1c**),[23] $Cp^*(OC)_2FeSiMe_3$ (**1d**),[24] $[Cp^*(OC)_2Fe]_2$,[25] $Cp^*(OC)_2FeH$,[26] $Cp^*(OC)_2RuMe$,[23] $HSiMe_2NR_2$ (R = Ph, *p*-Tol, and Et),[27] $ClSiMe_2OMe$,[28] and $ClGeMe_2NR_2$ (R = Ph and Me)[29] were prepared according to the literature methods. Other chemicals were purchased and used as received. NMR data were recorded on a Bruker ARX-300 or AV-300 spectrometer. $^{29}Si\{^1H\}$ NMR spectra were obtained by DEPT pulse sequence. IR spectra were recorded on a Horiba FT-730 spectrometer, mass spectra were measured using a JEOL JMS-HX110 or Hitachi M2500S spectrometer, and UV−visible spectra were recorded on a Shimadzu Multi Spec-1500 spectrometer. Irradiation was performed using an Ushio UM-452 450 W medium-pressure Hg lamp via a Pyrex glass filter at 5 °C.

Synthesis of $Cp^*(OC)(C_5H_5N)FeSiMe_2NPh_2$ (2a). Procedure A. A Pyrex tube (15 mm o.d.) equipped with a greaseless vacuum valve was charged with $Cp^*(OC)_2FeSiMe_2NPh_2$ (**1a**) (153 mg, 0.323 mmol) and connected to a vacuum line. Pyridine (2 mL, excess) and toluene (15 mL) were introduced into the tube under high vacuum by the trap-to-trap transfer technique. After sealing the tube off from the vacuum line, the contents were irradiated for 90 min. Degassing of the tube contents was performed using a vacuum line by the conventional freeze−pump−thaw technique every 30 min. The yellow solution gradually turned dark red as the reaction proceeded. After irradiation, volatiles were removed under reduced pressure, and the tube was flame-sealed. The tube was opened under N_2 in a glovebox, the residue extracted with toluene (3 mL × 3), and the dark red extract filtered through a Celite pad and concentrated in vacuo. Recrystallization of the residue from toluene/hexane (1:1) at −30 °C gave dark red crystals of **2a**. Yield: 122 mg (0.233 mmol, 72%); ^1H NMR (300 MHz, benzene-d_6): δ 0.59, 0.60 (s, 3H × 2, $SiMe_2$), 1.39 (s, 15H, C_5Me_5), 5.96 (t, $^3J_{HH}$ = 7.2 Hz, 2H, β-NC_5H_5), 6.44 (t, $^3J_{HH}$ = 7.2 Hz, 1H, γ-NC_5H_5), 6.88 (t, $^3J_{HH}$ = 7.2 Hz, 2H, *p*-NPh_2), 7.15 (t, $^3J_{HH}$ = 7.2 Hz, 4H, *m*-NPh_2), 7.22 (d, $^3J_{HH}$ = 7.2 Hz, 4H, *o*-NPh_2), 8.34 (d, $^3J_{HH}$ = 7.2 Hz, 2H, α-NC_5H_5); $^{13}C\{^1H\}$ NMR (75.5 MHz, benzene-d_6) δ 7.1, 8.3 ($SiMe_2$), 9.6 ($C_5\mathit{Me}_5$), 90.7 (C_5Me_5), 121.5 (β-NC_5H_5), 122.8 (*p*-NPh_2), 127.7 (*o*-NPh_2), 128.6 (*m*-NPh_2), 133.4 (γ-NC_5H_5), 153.1 (*ipso*-NPh_2), 157.1 (α-NC_5H_5), 225.4 (CO); $^{29}Si\{^1H\}$ NMR (59.6 MHz, benzene-d_6) δ 53.5; IR (benzene-d_6, cm^{-1}) 1878 (vs, ν_{CO}); EI-MS (70 eV) *m*/*z* 524 (11, M^+), 496 (15, $M^+ - CO$), 305 (84, $M^+ - Cp^* - Fe - CO$), 270 (13, $M^+ - CO - SiMe_2NPh_2$), 226 (100, $[SiMe_2NPh_2]^+$). Anal. Calcd for $C_{30}H_{36}FeN_2OSi$: C, 68.69; H, 6.92; N, 5.34. Found: C, 68.87; H, 7.12; N, 5.08.

Procedure B. Neat $HSiMe_2NPh_2$ (690 mg, 3.03 mmol) was added by syringe to a toluene solution of $Cp^*(OC)(C_5H_5N)FeMe$ (952 mg, 3.04 mmol) with stirring at room temperature. Immediate evolution of methane was confirmed. After stirring for 1 h, the insoluble materials were filtered off using a Celite pad and the filtrate was concentrated in vacuo to ca. 10 mL. The toluene solution was layered carefully with 10 mL of hexane. **2a** crystallized at −30 °C as dark red crystals. Yield: 1.15 g (2.19 mmol, 72%).

Synthesis of $Cp^*(OC)(C_5H_5N)FeSiMe_2NMe_2$ (2b). Complex **2b** (100 mg, 0.250 mmol) was synthesized as dark purple crystals in 61% yield by a method similar to that for **2a** (procedure A), using **1b** (144 mg, 0.412 mmol) and excess pyridine (2 mL). ^1H NMR (300 MHz, benzene-d_6) δ 0.43, 0.69 (s, 3H × 2, $SiMe_2$), 1.53 (s, 15H, C_5Me_5), 2.69 (s, 6H, NMe_2), 5.96 (d, $^3J_{HH}$ = 7.4 Hz, 2H, β-NC_5H_5), 6.47 (t, $^3J_{HH}$ = 7.4 Hz, 1H, γ-NC_5H_5), 8.46 (m, 2H, α-NC_5H_5); $^{13}C\{^1H\}$ NMR (75.5 MHz, benzene-d_6) δ 3.88, 3.93

(21) Homrighausen, C. L.; Alexander, J. J.; Bauer, J. A. K. *Inorg. Chim. Acta* **2002**, *334*, 419−436.
(22) Hashimoto, H.; Matsuda, A.; Tobita, H. *Chem. Lett.* **2005**, *34*, 1374−1375.
(23) Okazaki, M.; Satoh, K.; Akagi, T.; Iwata, M.; Jung, K. A.; Shiozawa, R.; Okada, H.; Ueno, K.; Tobita, H.; Ogino, H. *J. Organomet. Chem.* **2002**, *645*, 201−205.
(24) Randolph, C. L.; Wrighton, M. S. *Organometallics* **1987**, *6*, 365−371.
(25) Catheline, D.; Astruc, D. *Organometallics* **1984**, *3*, 1094−1100.
(26) Bullock, R. M.; Samsel, E. G. *J. Am. Chem. Soc.* **1990**, *112*, 6886−6898.
(27) (a) Tamao, K.; Nakajo, E.; Ito, Y. *Tetrahedron* **1988**, *44*, 3997−4007. (b) Tamao, K.; Kawachi, A.; Nakagawa, Y.; Ito, Y. *J. Organomet. Chem.* **1994**, *473*, 29−34. (c) Kawachi, A.; Tamao, K. *J. Am. Chem. Soc.* **2000**, *122*, 1919−1926.
(28) Hopper, S. P.; Tremelling, M. J.; Goldman, E. W. *J. Organomet. Chem.* **1978**, *156*, 331−340.
(29) Yoder, C. H.; Zuckerman, J. J. *J. Am. Chem. Soc.* **1966**, *88*, 4831−4839.

($SiMe_2$), 9.8 ($C_5\mathit{Me}_5$), 40.7 (NMe_2), 90.5 (C_5Me_5), 122.9 (β-NC_5H_5), 133.0 (γ-NC_5H_5), 156.7 (α-NC_5H_5), 224.1 (CO); $^{29}Si\{^1H\}$ NMR (59.6 MHz, benzene-d_6) δ 56.9; IR (benzene-d_6, cm^{-1}) 1869 (vs, ν_{CO}); EI-MS (70 eV) *m*/*z* 400 (12, M^+), 372 (14, $M^+ - CO$), 270 (25, $M^+ - CO - SiMe_2NMe_2$), 181 (88), 102 (100, $[SiMe_2NMe_2]^+$). Anal. Calcd for $C_{20}H_{32}FeN_2OSi$: C, 59.99; H, 8.06; N, 7.00. Found: C, 59.72; H, 8.19; N, 6.67.

Synthesis of Cp*(OC)Fe{η^3(*C*,*C*,*C*)-$C_5H_5NSiMe_2NPh_2$} (3a). A Pyrex tube (10 mm o.d.) equipped with a greaseless vacuum valve was charged with **2a** (40 mg, 76 μmol), and toluene (10 mL) was then introduced into this tube under high vacuum by the trap-to-trap transfer technique. The tube was flame-sealed, heated at 60 °C for 48 h, and then opened under N_2 in a glovebox. Volatiles were removed under reduced pressure, and the residue was extracted with pentane (5 mL × 2). The extract was filtered through a Celite pad. Cooling of the concentrated pentane solution at −30 °C afforded orange crystals of **3a**. Yield: 22 mg (42 μmol, 55%); ^1H NMR (300 MHz, benzene-d_6) δ 0.26, 0.34 (s, 3H × 2, $SiMe_2$), 1.50 (s, 15H, C_5Me_5), 1.77 (t, $^3J_{HH}$ = 5.4 Hz, 1H, H^2), 3.74 (t, $^3J_{HH}$ = 5.6 Hz, 1H, H^3), 5.30 (t, $^3J_{HH}$ = 6.3 Hz, 1H, H^4), 5.47 (d, $^3J_{HH}$ = 7.1 Hz, 1H, H^5), 5.73 (d, $^3J_{HH}$ = 5.3 Hz, 1H, H^1), 6.89 (t, $^3J_{HH}$ = 7.2 Hz, 2H, *p*-NPh_2), 7.06 (d, $^3J_{HH}$ = 7.2 Hz, 4H, *o*-NPh_2), 7.13 (t, $^3J_{HH}$ = 7.2 Hz, 4H, *m*-NPh_2); $^{13}C\{^1H\}$ NMR (75.5 MHz, benzene-d_6) δ −2.2, −1.1 ($SiMe_2$), 9.8 ($C_5\mathit{Me}_5$), 90.6 (C_5Me_5), 45.1 (C^2), 51.2 (C^3), 76.9 (C^1), 110.8 (C^4), 121.1 (C^5), 123.2 (*p*-NPh_2), 125.4 (*o*-NPh_2), 129.5 (*m*-NPh_2), 148.4 (*ipso*-NPh_2), 225.1 (CO); $^{29}Si\{^1H\}$ NMR (59.6 MHz, benzene-d_6) δ −2.3; IR (benzene-d_6, cm^{-1}) 1911 (vs, ν_{CO}); EI-MS (70 eV) *m*/*z* 524 (7, M^+), 496 (14, $M^+ - CO$), 402 (15, $M^+ - CO - Me - NC_5H_5$), 305 (75, $[C_5H_5NSiMe_2NPh_2]^+$), 270 (17, $M^+ - CO - SiMe_2NPh_2$), 226 (100, $[SiMe_2NPh_2]^+$). Anal. Calcd for $C_{30}H_{36}FeN_2OSi$: C, 68.69; H, 6.92; N, 5.34. Found: C, 68.75; H, 6.72; N, 5.41.

Monitoring the Thermal Reaction of Cp*(OC)(C_5H_5N)Fe$SiMe_2NMe_2$ (2b) by NMR Spectroscopy. A Pyrex NMR tube was charged with **2b** (1.0 mg, 2.5 μmol) and C_6Me_6 (0.5 mg, internal standard). Benzene-d_6 (0.7 mL) was then introduced into this tube under high vacuum by the trap-to-trap-transfer technique. The NMR tube was flame-sealed and then heated to 60 °C. The reaction was monitored by the ^1H NMR spectroscopy. The dark purple solution of **2b** gradually turned orange. After heating at 60 °C for 48 h, **3b** was obtained in 86% NMR yield: ^1H NMR (300 MHz, benzene-d_6) δ 0.17, 0.26 (s, 3H × 2, $SiMe_2$), 1.57 (s, 15H, C_5Me_5), 1.73 (t, $^3J_{HH}$ = 5.9 Hz, 1H, H^2), 2.45 (s, 6H, NMe_2), 3.76 (t, $^3J_{HH}$ = 5.5 Hz, 1H, H^3), 5.23−5.30 (m, 2H, H^4, H^5), 5.53 (d, $^3J_{HH}$ = 5.0 Hz, 1H, H^1); $^{13}C\{^1H\}$ NMR (75.5 MHz, benzene-d_6) δ −3.4, −3.3 ($SiMe_2$), 9.9 ($C_5\mathit{Me}_5$), 37.7 (NMe_2), 89.5 (C_5Me_5), 44.1 (C^2), 51.3 (C^3), 78.8 (C^1), 109.6 (C^4), 122.1 (C^5), 223.1 (CO); $^{29}Si\{^1H\}$ NMR (59.6 MHz, benzene-d_6) δ 0.3; IR (benzene-d_6, cm^{-1}) 1907 (vs, ν_{CO}); EI-MS (70 eV) *m*/*z* 400 (13, M^+), 372 (15, $M^+ - CO$), 270 (17, $M^+ - CO - SiMe_2NMe_2$), 181 (91), 102 (100, $[SiMe_2NMe_2]^+$).

Synthesis of Cp*(OC)(C_5H_5N)Fe$SiMe_2Cl$ (2c). Compound **2c** (204 mg, 0.521 mmol) was synthesized as orange crystals in 60% yield by a method similar to that for **2a** (procedure A), using **1c** (295 mg, 0.866 mmol) and pyridine (5 mL, excess). ^1H NMR (300 MHz, benzene-d_6) δ 0.44, 1.07 (s, 3H × 2, $SiMe_2$), 1.49 (s, 15H, C_5Me_5), 6.07 (br, 2H, β-NC_5H_5), 6.50 (t, $^3J_{HH}$ = 7.5 Hz, 1H, γ-NC_5H_5), 8.55 (br, 2H, α-NC_5H_5); $^{13}C\{^1H\}$ NMR (75.5 MHz, benzene-d_6) δ 9.5 ($C_5\mathit{Me}_5$), 9.9, 10.3 ($SiMe_2$), 91.4 (C_5Me_5), 123.7 (β-NC_5H_5), 134.6 (γ-NC_5H_5), 157.4 (br, α-NC_5H_5), 220.3 (CO); $^{29}Si\{^1H\}$ NMR (59.6 MHz, benzene-d_6) δ 99.0; IR (benzene-d_6, cm^{-1}) 1882 (vs, ν_{CO}); EI-MS (70 eV) *m*/*z* 391 (7, M^+), 284 (33, $M^+ - CO - NC_5H_5$), 190 (100, $M^+ - CO - NC_5H_5 - SiMe_2Cl - H$). Anal. Calcd for $C_{18}H_{26}ClFeNOSi$: C, 55.18; H, 6.69; N, 3.58. Found: C, 55.42; H, 6.82; N, 3.47.

Synthesis of Cp*(OC)(C_5H_5N)Fe$SiMe_3$ (2d). Compound **2d** (88 mg, 0.24 mmol) was synthesized as purple crystals in 46% yield by a method similar to that for **2a** (procedure A), using **1d** (166 mg, 0.518 mmol) and pyridine (2 mL, excess). ^1H NMR (300 MHz, benzene-d_6) δ 0.48 (s, 9H, $SiMe_3$), 1.52 (s, 15H, C_5Me_5), 5.98 (t, $^3J_{HH}$ = 7.4 Hz, 2H, β-NC_5H_5), 6.47 (t, $^3J_{HH}$ = 7.4 Hz, 1H, γ-NC_5H_5), 8.40 (br, 2H, α-NC_5H_5); $^{13}C\{^1H\}$ NMR (75.5 MHz, benzene-d_6) δ 4.8 ($SiMe_3$), 9.9 ($C_5\mathit{Me}_5$), 90.1 (C_5Me_5), 123.1 (β-NC_5H_5), 133.2 (γ-NC_5H_5), 156.7 (α-NC_5H_5), 222.5 (CO); $^{29}Si\{^1H\}$ NMR (59.6 MHz, benzene-d_6) δ 40.7; IR (benzene-d_6, cm^{-1}) 1873 (vs, ν_{CO}); EI-MS (70 eV) *m*/*z* 371 (3, M^+), 264 (18, $M^+ - CO - NC_5H_5$), 190 (100, $M^+ - CO - NC_5H_5 - SiMe_3 - H$). Anal. Calcd for $C_{19}H_{29}FeNOSi$: C, 61.45; H, 7.87; N, 3.77. Found: C, 61.07; H, 8.06; N, 3.83.

Synthesis of Cp*(OC)$_2$FeSiMe$_2$OMe (1e). An orange solution of Cp*(OC)$_2$FeH (1.23 g, 4.96 mmol) in diethyl ether (50 mL) was cooled to −45 °C and treated with *n*-BuLi (1.5 M hexane solution, 3.3 mL, 5.0 mmol). After stirring for 10 min at −45 °C, the mixture became an orange suspension. $ClSiMe_2OMe$ (1.07 g, 8.59 mmol) was added dropwise to the suspension at −45 °C, and the solution was subsequently allowed to warm to room temperature. After stirring for 12 h, volatiles were evaporated under reduced pressure, and the residue was extracted with hexane (10 mL × 3). The extract was filtered through a Celite pad, and then the filtrate was concentrated to dryness in vacuo. Purification of the residue by silica gel flash chromatography using toluene as an eluent gave two yellow bands. Evaporation of the solvent in vacuo from the first fraction and recrystallization of the residue from toluene/hexane (1:1) at −30 °C yielded yellow crystals of Cp*(OC)$_2$FeSiMe$_2$Cl (**1c**) (107 mg, 0.314 mmol, 6%). Evaporation of the solvent in vacuo from the second fraction afforded **1e** (752 mg, 2.24 mmol, 45%): ^1H NMR (300 MHz, benzene-d_6) δ 0.68 (s, 6H, $SiMe_2$), 1.56 (s, 15H, C_5Me_5), 3.44 (s, 3H, OMe); $^{13}C\{^1H\}$ NMR (75.5 MHz, benzene-d_6) δ 7.0 ($SiMe_2$), 9.7 ($C_5\mathit{Me}_5$), 50.6 (OMe), 95.2 (C_5Me_5), 217.7 (CO); $^{29}Si\{^1H\}$ NMR (59.6 MHz, benzene-d_6) δ 69.0; IR (benzene-d_6, cm^{-1}) 1975, 1919 (vs, ν_{CO}); EI-MS (70 eV) *m*/*z* 336 (47, M^+), 321 (7, $M^+ - Me$), 308 (44, $M^+ - CO$), 280 (100, $M^+ - 2CO$), 190 (79, $M^+ - 2CO - SiMe_2OMe - H$), 89 (19, $[SiMe_2OMe]^+$). Anal. Calcd for $C_{15}H_{24}FeO_3Si$: C, 53.57; H, 7.19. Found: C, 53.96; H, 7.46.

Synthesis of Cp*(OC)(C_5H_5N)Fe$SiMe_2OMe$ (2e). Compound **2e** (136 mg, 0.351 mmol) was synthesized as purple crystals in 50% yield by a method similar to that for **2a** (procedure A), using **1e** (237 mg, 0.705 mmol) and pyridine (2 mL, excess). ^1H NMR (300 MHz, benzene-d_6) δ 0.24, 0.72 (s, 3H × 2, $SiMe_2$), 1.52 (s, 15H, C_5Me_5), 3.63 (s, 3H, OMe), 6.07 (t, $^3J_{HH}$ = 6.9 Hz, 2H, β-NC_5H_5), 6.53 (t, $^3J_{HH}$ = 6.9 Hz, 1H, γ-NC_5H_5), 8.59 (d, $^3J_{HH}$ = 6.9 Hz, 2H, α-NC_5H_5); $^{13}C\{^1H\}$ NMR (75.5 MHz, benzene-d_6) δ 3.4, 4.2 ($SiMe_2$), 9.8 ($C_5\mathit{Me}_5$), 50.9 (OMe), 90.6 (C_5Me_5), 123.2 (β-NC_5H_5), 133.7 (γ-NC_5H_5), 156.6 (br, α-NC_5H_5), 222.0 (CO); $^{29}Si\{^1H\}$ NMR (59.6 MHz, benzene-d_6) δ 77.4; IR (benzene-d_6, cm^{-1}) 1873 (vs, ν_{CO}); EI-MS (70 eV) *m*/*z* 387 (27, M^+), 308 (50, $M^+ - NC_5H_5$), 280 (100, $M^+ - CO - NC_5H_5$), 190 (39, $M^+ - CO - NC_5H_5 - SiMe_2OMe - H$). Anal. Calcd for $C_{19}H_{29}FeNO_2Si$: C, 58.91; H, 7.55; N, 3.62. Found: C, 58.41; H, 7.70; N, 3.53.

Monitoring the Thermal Reaction of Cp*(OC)(C_5H_5N)Fe$SiMe_2$R (R = Cl (2c), Me, (2d), OMe (2e)). For **2c**: Heating at 60 °C did not result in changes in the ^1H NMR spectrum. After heating for 24 h at 90 °C, **2c** was recovered in 79% NMR yield with the formation of $[Cp^*(OC)_2Fe]_2$ (6%) and Cp^*_2Fe (3%). Prolonged heating led to decomposition, and the NMR signals characteristic of the pyridine-insertion product were not detected. For **2d**: Heating at 60 °C did not result in changes in the ^1H NMR spectrum. After heating for 24 h at 90 °C, unidentified broad signals were observed in the ^1H NMR spectrum, where **2d** remained in 40% NMR yield and the NMR signals characteristic of the pyridine-insertion product were not detected. For **2e**: Heating at 60 °C did not result in changes in the ^1H NMR spectrum. After heating for 24 h at 90 °C, the formation of Cp*(OC)Fe{η^3(*C*,*C*,*C*)-C_5H_5-

$NSiMe_2OMe$} (**3e**) was confirmed in 18% NMR yield together with $Me_2Si(OMe)_2$ (24%) and the recovered **2e** (9%). Weak unidentified signals were also observed. Prolonged heating for 36 h at 90 °C resulted in the complete disappearance of **2e** to afford **3e** and $Me_2Si(OMe)_2$ in yields of 16% and 28%, respectively. **3e**: ^{1}H NMR (300 MHz, benzene-d_6) δ 0.12, 0.31 (s, 3H × 2, $SiMe_2$), 1.53 (s, 15H, C_5Me_5), 3.39 (s, 3H, OMe), 1.79 (br, 1H, H^2), 3.70 (br, 1H, H^3), 5.21 (br, 1H, H^4), 5.32 (br, 1H, H^5), 5.62 (br, 1H, H^1); ^{13}C{^{1}H} NMR (75.5 MHz, benzene-d_6) δ −3.4, −1.4 ($SiMe_2$), 10.0 (C_5Me_5), 50.2 (OMe), 45.5 (C^2), 51.0 (C^3), 77.9 (C^1), 110.3 (C^4), 121.5 (C^5); ^{29}Si{^{1}H} NMR (75.5 MHz, benzene-d_6) δ 2.2.

Synthesis of Cp*(OC)$_2$FeGeMe$_2$NPh$_2$ (1f). To a solution of $ClGeMe_2NPh_2$ (550 mg, 1.80 mmol) in tetrahydrofuran (THF; 20 mL) was added a solution of K[Cp*(OC)$_2$Fe] in THF (20 mL), which was prepared by reduction of [Cp*(OC)$_2$Fe]$_2$ (510 mg, 1.03 mmol) with Na/K alloy (Na, 95 mg, 4.1 mmol; K, 483 mg, 12.4 mmol). The reaction mixture was stirred at −45 °C for 30 min, allowed to warm to room temperature, and stirred for a further 2 h. Volatiles were removed under reduced pressure, and the residue was extracted with hexane (10 mL × 3). The extract was filtered through a Celite pad and concentrated under reduced pressure. Recrystallization of the residue from hexane at −75 °C afforded yellow crystals of **1f**. Yield: 542 mg (1.05 mmol, 58%); ^{1}H NMR (300 MHz, benzene-d_6) δ 0.74 (s, 6H, $GeMe_2$), 1.39 (s, 15H, C_5Me_5), 6.90 (t, $^3J_{HH}$ = 7.2 Hz, 2H, *p*-Ph), 7.15−7.26 (m, 8H, *o*,*m*-Ph); ^{13}C{^{1}H} NMR (75.5 MHz, benzene-d_6) δ 9.6 ($GeMe_2$), 9.8 (C_5Me_5), 95.3 (C_5Me_5), 121.0 (*p*-Ph), 125.6 (*o*-Ph), 129.2 (*m*-Ph), 152.7 (*ipso*-Ph), 217.9 (CO); IR (KBr, cm^{-1}) 1975, 1936 (vs, ν_{CO}). Anal. Calcd for $C_{26}H_{31}FeGeNO_2$: C, 60.29; H, 6.03; N, 2.70. Found: C, 60.19; H, 6.38; N, 2.53.

Synthesis of Cp*(OC)$_2$FeGeMe$_2$NMe$_2$ (1g). Compound **1g** (1.23 g, 3.12 mmol) was synthesized as light red crystals in 69% yield by a method similar to that for **1f**, using [Cp*(OC)$_2$Fe]$_2$ (1.11 g, 2.25 mmol), Na/K alloy (Na, 156 mg, 6.78 mmol; K, 794 mg, 20.3 mmol), and $ClGeMe_2NMe_2$ (1.03 g, 5.65 mmol). ^{1}H NMR (300 MHz, benzene-d_6) δ 0.68 (s, 6H, $GeMe_2$), 1.54 (s, 15H, C_5Me_5), 2.70 (s, 6H, NMe_2); ^{13}C{^{1}H} NMR (75.5 MHz, benzene-d_6) δ 4.8 ($GeMe_2$), 9.9 (C_5Me_5), 42.4 (NMe_2), 94.9 (C_5Me_5), 218.2 (CO); IR (benzene-d_6, cm^{-1}) 1973, 1917 (vs, ν_{CO}). Anal. Calcd for $C_{16}H_{27}FeGeNO_2$: C, 48.79; H, 6.91; N, 3.56. Found: C, 48.41; H, 6.91; N, 2.91.

Synthesis of Cp*(OC)$_2$FeGeMe$_3$ (1h). Compound **1h** (739 mg, 2.03 mmol) was synthesized as orange needles in 51% yield by a method similar to that for **1f**, using [Cp*(OC)$_2$Fe]$_2$ (986 mg, 2.00 mmol), Na/K alloy (Na, 108 mg, 4.70 mmol; K, 586 mg, 15.0 mmol), and $BrGeMe_3$ (1.54 g, 7.79 mmol). ^{1}H NMR (300 MHz, benzene-d_6) δ 0.66 (s, 9H, $GeMe_3$), 1.50 (s, 15H, C_5Me_5); ^{13}C{^{1}H} NMR (75.5 MHz, benzene-d_6) δ 5.6 ($GeMe_3$), 9.9 (C_5Me_5), 94.2 (C_5Me_5), 218.1 (CO); IR (KBr pellet, cm^{-1}) 1968, 1905 (vs, ν_{CO}). Anal. Calcd for $C_{15}H_{24}FeGeO_2$: C, 49.39; H, 6.63. Found: C, 49.48; H, 6.58.

Synthesis of Cp*(OC)(C$_5$H$_5$N)FeGeMe$_2$NPh$_2$ (2f). Compound **2f** (197 mg, 0.346 mmol) was synthesized as purple crystals in 60% yield by a method similar to that for **2a** (procedure A), using **1f** (300 mg, 0.579 mmol) and pyridine (5 mL, excess). ^{1}H NMR (300 MHz, benzene-d_6) δ 0.68 (s, 6H, $GeMe_2$), 1.37 (s, 15H, C_5Me_5), 6.00 (t, $^3J_{HH}$ = 6.9 Hz, 2H, β-NC_5H_5), 6.46 (t, $^3J_{HH}$ = 6.9 Hz, 1H, γ-NC_5H_5), 6.82 (t, $^3J_{HH}$ = 7.2 Hz, 2H, *p*-Ph), 7.00 (t, $^3J_{HH}$ = 7.2 Hz, 4H, *m*-Ph), 7.15 (d, $^3J_{HH}$ = 7.2 Hz, 4H, *o*-Ph), 8.34 (d, $^3J_{HH}$ = 6.9 Hz, 2H, α-NC_5H_5); ^{13}C{^{1}H} NMR (75.5 MHz, benzene-d_6) δ 7.7, 8.1 ($GeMe_2$), 9.8 (C_5Me_5), 90.0 (C_5Me_5), 119.6 (β-NC_5H_5), 123.0 (*p*-Ph), 125.3 (*o*-Ph), 128.7 (*m*-Ph), 134.3 (γ-NC_5H_5), 153.8 (*ipso*-Ph), 157.5 (α-NC_5H_5), 224.4 (CO); IR (benzene-d_6, cm^{-1}) 1888 (vs, ν_{CO}). Anal. Calcd for $C_{30}H_{36}FeGeN_2O$: C, 63.32; H, 6.38; N, 4.92. Found: C, 62.95; H, 6.61; N, 4.80.

Synthesis of Cp*(OC)(C$_5$H$_5$N)FeGeMe$_2$NMe$_2$ (2g). Compound **2g** (143 mg, 0.321 mmol) was synthesized as dark purple crystals in 63% yield by a method similar to that for **2a** (procedure A), using **1g** (200 mg, 0.508 mmol) and pyridine (5 mL, excess). ^{1}H NMR (300 MHz, benzene-d_6) δ 0.50, 0.75 (s, 3H × 2, $GeMe_2$), 1.50 (s, 15H, C_5Me_5), 2.77 (s, 6H, NMe_2), 6.00 (t, $^3J_{HH}$ = 6.6 Hz, 2H, β-NC_5H_5), 6.49 (t, $^3J_{HH}$ = 6.6 Hz, 1H, γ-NC_5H_5), 8.44 (d, $^3J_{HH}$ = 6.6 Hz, 2H, α-NC_5H_5); ^{13}C{^{1}H} NMR (75.5 MHz, benzene-d_6) δ 1.6, 3.1 ($GeMe_2$), 9.9 (C_5Me_5), 43.3 (NMe_2), 89.8 (C_5Me_5), 123.3 (β-NC_5H_5), 134.0 (γ-NC_5H_5), 157.4 (α-NC_5H_5), 224.2 (CO); IR (benzene-d_6, cm^{-1}) 1877 (vs, ν_{CO}). Anal. Calcd for $C_{20}H_{32}FeGeN_2O$: C, 53.99; H, 7.25; N, 6.30. Found: C, 53.55; H, 7.17; N, 5.76.

Synthesis of Cp*(OC)(C$_5$H$_5$N)FeGeMe$_3$ (2h). Compound **2h** (242 mg, 0.582 mmol) was synthesized as dark purple crystals in 71% yield by a method similar to that for **2a** (procedure A), using **1h** (300 mg, 0.822 mmol) and pyridine (2 mL, excess). ^{1}H NMR (300 MHz, benzene-d_6) δ 0.53 (s, 9H, $GeMe_3$), 1.50 (s, 15H, C_5Me_5), 6.00 (t, $^3J_{HH}$ = 6.9 Hz, 2H, β-NC_5H_5), 6.49 (t, $^3J_{HH}$ = 6.9 Hz, 1H, γ-NC_5H_5), 8.44 (d, $^3J_{HH}$ = 6.9 Hz, 2H, α-NC_5H_5); ^{13}C{^{1}H} NMR (75.5 MHz, benzene-d_6) δ 3.3 ($GeMe_3$), 9.9 (C_5Me_5), 89.2 (C_5Me_5), 123.1 (β-NC_5H_5), 133.6 (γ-NC_5H_5), 156.6 (α-NC_5H_5), 223.0 (CO); IR (benzene-d_6, cm^{-1}) 1876 (vs, ν_{CO}). Anal. Calcd for $C_{19}H_{29}FeGeNO$: C, 54.87; H, 7.03; N, 3.37. Found: C, 54.99; H, 7.07; N, 3.21.

Monitoring the Thermal Reaction of Cp*(OC)(C$_5$H$_5$N)FeGeMe$_2$R (R = NPh$_2$ (2f), NMe$_2$ (2g), Me (2h)). For **2f**: Heating at 60 °C did not result in changes in the ^{1}H NMR spectrum. After heating for 24 h at 110 °C, **2f** remained in 70% NMR yield, and several weak unidentified signals emerged in the ^{1}H NMR spectrum. However, the pyridine-insertion products were not detected at all. For **2g**: Heating at 60 °C did not produce changes in the ^{1}H NMR spectrum. Heating at 80 °C caused the signals of **2g** to weaken gradually, and prolonged heating for 8 h at 80 °C resulted in the disappearance of **2g** to afford unidentified products with the release of free pyridine. The pyridine-insertion product was not observed in the ^{1}H NMR spectrum. For **2h**: Heating at 60 °C did not result in changes in the ^{1}H NMR spectrum. After heating for 24 h at 110 °C, **2h** was recovered in 75% NMR yield accompanied by the formation of [Cp*(OC)$_2$Fe]$_2$ (5% NMR yield). The NMR signals characteristic of the pyridine-insertion product were not detected.

Kinetic Study of Thermal Conversion from Cp*(OC)(C$_5$H$_5$N)FeSiMe$_2$NPh$_2$ (2a) to Cp*(OC)Fe{η^3(*C*,*C*,*C*)-C$_5$H$_5$NSiMe$_2$NPh$_2$} (3a). A 10 mL volumetric flask was charged with **2a** (103 mg, 0.196 mmol) and C_6Me_6 (9.0 mg, internal standard). Benzene-d_6 was added to the flask to make the volume of the solution up to 10.0 mL. Five NMR tubes were filled with this solution (1.96 × 10^{-3} M) and flame-sealed under high vacuum. The samples were heated at five different temperatures (328, 333, 338, 343, and 348 K) in an oil bath. Thermal conversion from **2a** to **3a** was periodically monitored by ^{1}H NMR spectroscopy. A linear correlation was found between $\ln(A_t/A_0)$ and time, where A_0 and A_t are the molar fractions of **2a** at time 0 and t (see Supporting Information).

Synthesis of Cp*(OC)(C$_5$H$_5$N)RuMe. A Pyrex tube (20 mm o.d.) equipped with a greaseless vacuum valve was charged with Cp*(OC)$_2$RuMe (398 mg, 1.29 mmol) and connected to a vacuum line. Pyridine (1 mL, excess) and hexane (15 mL) were introduced into this tube under high vacuum by the trap-to-trap transfer technique. After sealing the tube off from the vacuum line, the solution was irradiated for 3 h. Degassing of the solution was performed using a vacuum line by the conventional freeze−pump−thaw technique every 30 min. The light red solution gradually turned dark orange as the reaction proceeded. After irradiation, volatiles were removed under reduced pressure, and the tube was reopened under N_2 in a glovebox. The residue was extracted with hexane (5 mL × 3), the dark orange extract was filtered through a Celite pad, and the filtrate was concentrated in vacuo. Recrystallization of the residue from hexane at −30 °C gave dark orange crystals of Cp*-

(OC)(C_5H_5N)RuMe. Yield: 343 mg (0.957 mmol, 74%); ^{1}H NMR (300 MHz, benzene-d_6) δ 0.59 (s, 3H, RuMe), 1.60 (s, 15H, C_5Me_5), 6.15 (t, $^3J_{HH}$ = 6.9 Hz, 2H, β-NC_5H_5), 6.58 (t, $^3J_{HH}$ = 6.9 Hz, 1H, γ-NC_5H_5), 8.26 (d, $^3J_{HH}$ = 6.9 Hz, 2H, α-NC_5H_5); ^{13}C{^{1}H} NMR (75.5 MHz, benzene-d_6) δ −7.0 (RuMe), 9.7 (C_5Me_5), 92.2 (C_5Me_5), 123.9 (β-NC_5H_5), 134.3 (γ-NC_5H_5), 155.9 (α-NC_5H_5), 210.3 (CO); IR (benzene-d_6, cm^{-1}) 1884 (ν_{CO}). Anal. Calcd for $C_{17}H_{23}NORu$: C, 56.96; H, 6.47; N, 3.91. Found: C, 56.93; H, 6.38; N, 3.85.

Reaction of Cp*(OC)(C_5H_5N)RuMe with $HSiMe_2NPh_2$. A Pyrex tube (20 mm o.d.) equipped with a greaseless vacuum valve was charged with Cp*(OC)(C_5H_5N)RuMe (370 mg, 1.03 mmol) and $HSiMe_2NPh_2$ (230 mg, 1.01 mmol). Toluene (15 mL) was then introduced into this tube under high vacuum by the trap-to-trap transfer technique. The solution was stirred at room temperature for 6 h, after which volatiles were removed in vacuo. The NMR spectroscopic data indicated a 5:4 mixture of Cp*(OC)(C_5H_5N)-$RuSiMe_2NPh_2$ (**2i**) and Cp*(OC)HRu{κ^2(*Si,C*)-$SiMe_2N$(*o*-C_6H_4)-(Ph)} (**4i**). Recrystallization of the residue from toluene/pentane (1:1) at −30 °C afforded **2i** as orange crystals and **4i** as light yellow crystals, which were separated on the basis of color. Yield of **2i**: 170 mg (0.298 mmol, 29%). Yield of **4i**: 155 mg (0.316 mmol, 31%). Data for **2i**: ^{1}H NMR (300 MHz, benzene-d_6) δ 0.47, 0.61 (s, 3H × 2, $SiMe_2$), 1.55 (s, 15H, C_5Me_5), 6.11 (t, $^3J_{HH}$ = 6.9 Hz, 2H, β-NC_5H_5), 6.56 (t, $^3J_{HH}$ = 6.9 Hz, 1H, γ-NC_5H_5), 6.86−6.91 (m, 2H, *p*-Ph), 7.12−7.17 (m, 8H, *o,m*-Ph), 8.29 (d, $^3J_{HH}$ = 6.9 Hz, 2H, α-NC_5H_5); ^{13}C{^{1}H} NMR (75.5 MHz, benzene-d_6) δ 6.6, 8.4 ($SiMe_2$), 10.0 (C_5Me_5), 94.8 (C_5Me_5), 121.1 (β-NC_5H_5), 123.4 (*p*-Ph), 126.8 (*o*-Ph), 128.7 (*m*-Ph), 133.9 (γ-NC_5H_5), 152.7 (*ipso*-Ph), 156.2 (α-NC_5H_5), 211.7 (CO); ^{29}Si{^{1}H} NMR (59.6 MHz, benzene-d_6) 37.8; IR (benzene-d_6, cm^{-1}) 1890 (vs, ν_{CO}). Anal. Calcd for $C_{30}H_{36}N_2ORuSi$: C, 63.24; H, 6.37; N, 4.92. Found: C, 63.57; H, 6.40; N, 4.79. Data for **4i**: ^{1}H NMR (benzene-d_6, 300 MHz, 298 K) δ −10.53 (br, 1H, RuH), 0.53, 0.56 (s, 3H × 2, $SiMe_2$), 1.49 (s, 15H, C_5Me_5), 6.80 (t, $^3J_{HH}$ = 7.5 Hz, aromatic), 7.00 (m, aromatic), 7.20−7.28 (m, aromatic); ^{1}H NMR (toluene-d_8, 253 K) δ −10.53 (s, 1H, RuH), 0.55, 0.60 (s, 3H × 2, SiMe), 1.44 (s, 15H, C_5Me_5), 6.84 (t, $^3J_{HH}$ = 6.9 Hz, 2H, aromatic), 7.14 (s, 3H, aromatic), 7.27 (t, $^3J_{HH}$ = 7.5 Hz, 3H, aromatic), 7.48 (d, $^3J_{HH}$ = 7.2 Hz, 1H, aromatic); ^{13}C{^{1}H} NMR (benzene-d_6, 75.5 MHz, 298 K) δ 4.9, 9.9 (SiMe), 100.7 (C_5Me_5), 120.5, 123.7, 126.9, 129.7, 146.3, 159.0 (aromatic), 205.4 (CO); (toluene-d_8, 253 K) δ 4.7, 9.75 (SiMe), 9.84 (C_5Me_5), 100.3 (C_5Me_5), 112.1, 120.3, 123.2, 125.6, 127.2, 129.5, 136.2, 143.1, 146.0, 158.3 (aromatic), 205.3 (CO); ^{29}Si{^{1}H} NMR (benzene-d_6, 59.6 MHz, 298 K) δ 52.2; IR (benzene-d_6, cm^{-1}) 1973 (ν_{CO}). Anal. Calcd for $C_{25}H_{31}NORuSi$: C, 61.19; H, 6.37; N, 2.85. Found: C, 61.47; H, 6.32; N, 2.78.

Reaction of Cp*(OC)(C_5H_5N)RuMe with $HSiMe_2N$(*p*-Tol)$_2$. This reaction was carried out by a method similar to that employed for $HSiMe_2NPh_2$, in this case using Cp*(OC)(C_5H_5N)RuMe (288 mg, 0.803 mmol) and $HSiMe_2N$(*p*-Tol)$_2$ (198 mg, 0.775 mmol). After 6 h at room temperature, the NMR spectroscopic data indicated a 1:1 mixture of Cp*(OC)(C_5H_5N)$RuSiMe_2N$(*p*-Tol)$_2$ (**2j**) and Cp*(OC)HRu{κ^2(*Si,C*)-$SiMe_2N$(*o*-C_6H_3(4-Me))(*p*-Tol)} (**4j**). Recrystallization of the residue from toluene/pentane (1:1) at −30 °C gave yellow crystals of **4j**. Yield: 134 mg (0.258 mmol, 33%); ^{1}H NMR (benzene-d_6, 300 MHz, 298 K) δ −10.51 (br, 1H, RuH), 0.58, 0.60 (s, 3H × 2, $SiMe_2$), 1.52 (s, 15H, C_5Me_5), 2.19, 2.29 (s, 3H × 2, *p*-Me), 7.08−7.19 (m, aromatic); ^{1}H NMR (toluene-d_8, 300 MHz, 258 K) δ −10.51 (s, 1H, RuH), 0.59, 0.62 (s, 3H × 2, $SiMe_2$), 1.51 (s, 15H, C_5Me_5), 2.21, 2.32 (s, 3H × 2, *p*-Me), 6.76 (m, 2H, aromatic), 7.01 (s, 1H, aromatic), 7.10 (s, 1H, aromatic), 7.17 (m, 2H, aromatic), 7.35 (m, 1H, aromatic); ^{13}C{^{1}H} NMR (benzene-d_6, 75.5 MHz, 298 K) δ 4.7, 9.7 (SiMe), 10.0 (C_5Me_5), 20.8, 21.0 (*p*-Me), 100.5 (C_5Me_5), 126.7, 130.2, 132.6, 143.7, 156.7 (aromatic), 205.4 (CO); (toluene-d_8, 253 K) δ 4.8, 9.9 (SiMe), 10.1 (C_5Me_5), 20.3, 21.0 (*p*-Me), 100.5 (C_5Me_5), 111.8, 126.4, 130.3, 132.4, 136.2, 143.8, 144.2, 156.5 (aromatic), 205.7 (CO); ^{29}Si{^{1}H} NMR (benzene-d_6, 59.6 MHz, 298 K) δ 50.9; IR (benzene-d_6, cm^{-1}) 1971 (ν_{CO}). Anal. Calcd. for $C_{27}H_{35}NORuSi$: C, 62.52; H, 6.80; N, 2.70. Found: C, 62.79; H, 6.75; N, 2.90.

Thermal Reaction of Cp*(OC)(C_5H_5N)RuMe with $HSiMe_2NPh_2$ in the Presence of Excess Pyridine. A Pyrex tube (15 mm o.d.) equipped with a greaseless vacuum valve was charged with Cp*(OC)(C_5H_5N)RuMe (125 mg, 0.349 mmol) and $HSiMe_2$-NPh_2 (80 mg, 0.35 mmol). Toluene (5 mL) and pyridine (215 mg, 2.72 mmol) were then introduced into this tube under high vacuum by the trap-to-trap transfer technique. The tube was sealed, heated at 80 °C for 12 h, and then opened under N_2 in a glovebox. Volatiles were removed under reduced pressure. The NMR spectroscopic data of the residue revealed selective formation of Cp*(OC)(C_5H_5N)-$RuSiMe_2NPh_2$ (**2i**). Recrystallization of the residue from toluene/hexane (1:1) at −30 °C gave light yellow crystals of **2i**. Yield: 143 mg (0.251 mmol, 72%).

Thermal Reaction of Cp*(OC)(C_5H_5N)RuMe with $HSiMe_2NEt_2$ in the Presence of Excess Pyridine. This reaction was carried out by a method similar to that employed for $HSiMe_2NPh_2$, in this case using Cp*(OC)(C_5H_5N)RuMe (112 mg, 0.313 mmol), $HSiMe_2NEt_2$ (40 mg, 0.30 mmol), and pyridine (147 mg, 1.86 mmol). After stirring at 80 °C for 12 h, volatiles were removed under reduced pressure, and the residue was extracted with hexane (3 mL × 3). The extract was filtered through a Celite pad. Cooling of the concentrated filtrate at −30 °C afforded a yellow powder of Cp*-(OC)(C_5H_5N)$RuSiMe_2NEt_2$ (**2k**). Yield: 55 mg (0.12 mmol, 38%); ^{1}H NMR (300 MHz, benzene-d_6) δ 0.27, 0.55 (s, 3H × 2, $SiMe_2$), 1.25 (t, $^3J_{HH}$ = 6.9 Hz, 6H, $N(CH_2CH_3)_2$), 1.69 (s, 15H, C_5Me_5), 3.14, 3.22 (q, $^3J_{HH}$ = 6.9 Hz, 2H × 2, $N(CH_2CH_3)_2$), 6.07 (t, $^3J_{HH}$ = 6.9 Hz, 2H, β-NC_5H_5), 6.54 (t, $^3J_{HH}$ = 6.9 Hz, 1H, γ-NC_5H_5), 8.38 (d, $^3J_{HH}$ = 6.9 Hz, 2H, α-NC_5H_5); ^{13}C{^{1}H} NMR (75.5 MHz, benzene-d_6) δ 4.2, 6.8 ($SiMe_2$), 10.3 (C_5Me_5), 16.4 ($N(CH_2CH_3)_2$), 41.9 ($N(CH_2CH_3)_2$), 94.5 (C_5Me_5), 124.0 (β-NC_5H_5), 133.7 (γ-NC_5H_5), 156.2 (α-NC_5H_5), 211.4 (CO); ^{29}Si{^{1}H} NMR (59.6 MHz, benzene-d_6) δ 41.5; IR (benzene-d_6, cm^{-1}) 1882 (vs, ν_{CO}). Anal. Calcd for $C_{22}H_{36}N_2ORuSi$: C, 55.78; H, 7.66; N, 5.91. Found: C, 55.23; H, 7.34; N, 5.31.

Monitoring the Thermal Reaction of Cp*(OC)(C_5H_5N)-$RuSiMe_2NR_2$ (R = Ph (2i), Et (2k)). For **2i**: To a Pyrex NMR tube was added a benzene-d_6 solution (0.7 mL) of **2i** (10 mg, 18 μmol) and C_6Me_6 (0.5 mg, internal standard). The NMR tube was flame-sealed under high vacuum. The reaction at 25 °C was monitored by ^{1}H NMR spectroscopy. After 5 h, an equilibrium between **2i** and **4i** was attained at a 1:1 molar ratio. The equilibrium mixture was heated at 100 °C while monitoring by ^{1}H NMR spectroscopy. After 48 h, the equilibrium had shifted to the side of **4i**, giving a 2:9 mixture of **2i** and **4i**. However, the pyridine-insertion product was not observed in the ^{1}H NMR spectrum. For **2k**: Heating at 60 °C did not result in changes in the ^{1}H NMR spectrum. After heating for 4 h at 80 °C, several unidentified signals emerged in the ^{1}H NMR spectrum, but **2k** remained in 18% NMR yield. The NMR signals of the pyridine-insertion product were not observed.

Synthesis of Cp*Fe(η^5-$C_5H_5NSiMe_2NPh_2$) (5a). A Pyrex sample tube (20 mm o.d.) with a greaseless vacuum valve was charged with **3a** (123 mg, 0.234 mmol) and connected to a vacuum line. Toluene (25 mL) was then introduced into the tube under high vacuum by the trap-to-trap transfer technique. After sealing the tube off from the vacuum line, the solution was irradiated for 30 min. The tube was subsequently reopened under N_2 in glovebox. After evaporation of volatiles under reduced pressure, the residue was extracted with pentane (5 mL × 2), and the extract was filtered through a Celite pad. Cooling of the concentrated filtrate (ca. 3 mL) at −30 °C afforded orange crystals of **5a**. Yield: 83 mg (0.17 mmol, 71%). ^{1}H NMR (300 MHz, benzene-d_6) δ −0.02 (s, 6H, $SiMe_2$), 1.67 (s, 15H, C_5Me_5), 2.67 (d, $^3J_{HH}$ = 3.0 Hz, 2H,

Table 1. Crystallographic Data of 2a, 3a, 4j, and 5a

	2a	3a	4j	5a
formula	$C_{30}H_{36}FeN_2OSi$	$C_{30}H_{36}FeN_2OSi$	$C_{27}H_{35}NORuSi$	$C_{29}H_{36}FeN_2Si$
cryst size (mm)	0.30 × 0.30 × 0.30	0.20 × 0.20 × 0.20	0.30 × 0.30 × 0.20	0.30 × 0.30 × 0.10
fw	524.56	524.56	518.72	496.55
cryst syst	monoclinic	monoclinic	monoclinic	monoclinic
space group	$P2_1/n$ (No. 14)	$P2_1/a$ (No. 14)	$C2/c$ (No. 15)	$P2_1/n$ (No. 14)
a (Å)	11.4245(4)	17.1694(6)	40.5980(10)	16.1381(4)
b (Å)	16.9079(5)	9.0939(4)	8.70160(10)	10.0021(4)
c (Å)	16.8660(3)	18.5947(6)	15.1845(2)	16.4567(7)
b (deg)	92.431(2)	109.099(2)	107.912(2)	100.529(1)
V (Å^3)	2676.0(1)	2743.5(2)	5104.18(15)	2611.6(2)
Z	4	4	8	4
F_{000}	1112	1112	2160	1056
μ(Mo Kα) (cm^{-1})	6.33	6.18	6.79	6.42
no. of reflns collected	25124	26166	16824	23665
no. of indep reflns (R_{int})	6298 (0.039)	6255 (0.056)	5707 (0.064)	6265 (0.039)
max. and min. transmn	0.77 and 0.87	0.81 and 0.90	0.83 and 0.88	0.76 and 0.90
no. of variables	316	316	289	298
R, R_w	0.060, 0.119	0.070, 0.132	0.080, 0.198	0.061, 0.121
R_1 [$I > 2\sigma(I)$]	0.033	0.051	0.062	0.033
no. of reflns to calc R_1	5370	4963	4671	5271
GOF	0.99	1.41	1.13	1.02
largest diff peak and hole (e Å^{-3})	0.25 and −0.51	0.79 and −0.71	0.90 and −2.02	0.29 and −0.27

α-NC_5H_5), 3.36 (m, 2H, β-NC_5H_5), 5.48 (t, $^3J_{HH}$ = 4.8 Hz, 1H, γ-NC_5H_5), 6.93 (t, $^3J_{HH}$ = 7.2 Hz, 2H, *p*-Ph), 7.10 (d, $^3J_{HH}$ = 7.2 Hz, 4H, *o*-Ph), 7.19 (t, $^3J_{HH}$ = 7.2 Hz, 4H, *m*-Ph); $^{13}C\{^1H\}$ NMR (75.5 MHz, benzene-d_6) δ −2.8 ($SiMe_2$), 10.5 (C_5Me_5), 45.2 (α-NC_5H_5), 78.5 (β-NC_5H_5), 85.0 (γ-NC_5H_5), 90.6 (C_5Me_5), 122.5 (*p*-Ph), 125.4 (*o*-Ph), 129.2 (*m*-Ph), 149.0 (*ipso*-Ph); $^{29}Si\{^1H\}$ NMR (59.6 MHz, benzene-d_6) δ −14.2 ($SiMe_2$); IR (benzene-d_6, cm^{-1}) no band for CO region; EI-MS (70 eV) *m*/*z* 496 (100, M^+), 402 (42, $M^+ - Me - NC_5H_5$), 305 (4, $[C_5H_5NSiMe_2NPh_2]^+$), 283 (39), 270 (46, $M^+ - SiMe_2NPh_2$), 226 (34, $[SiMe_2NPh_2]^+$). Anal. Calcd for $C_{29}H_{36}FeN_2Si$: C, 70.15; H, 7.31; N, 5.64. Found: C, 69.83; H, 7.52; N, 5.68.

X-ray Crystal Structure Determination of 2a, 3a, 4j, and 5a. Single crystals of **2a**, **3a**, **4j**, and **5a** were obtained by cooling the solutions at −30 °C. Intensity data for X-ray crystal structure analysis were collected at 150 K using a Rigaku RAXIS-RAPID imaging plate diffractometer with graphite-monochromated Mo Kα radiation. The data were corrected for Lorentz−polarization effects, and numerical absorption corrections were applied on each crystal shape. The structures of **2a**, **3a**, and **5a** were solved by heavy-atom Patterson methods (PATTY) and expanded using Fourier techniques (DIRDIF-94).[30] All calculations were performed using the teXsan crystallographic software package (Molecular Structure Corporation). The structure of **4j** was solved by Patterson and Fourier transform methods using SHELXS-97 and refined by full matrix least-squares techniques on all F^2 data (SHELXL-97).[31] All non-hydrogen atoms were located and refined anisotropically. Hydrogen atoms were placed at their geometrically calculated positions. Details of the data collection and refinement are provided in Table 1.

Supporting Information Available: Kinetic data for the isomerization from **2a** to **3a** and CIF files for all crystal structures. This material is available free of charge via the Internet at http://pubs.acs.org.

OM060873N

(30) Beurskens, P. T.; Admiraal, G.; Beurskens, G.; Bosman, W. P.; De Gelder, R.; Israel, R.; M. Smits, J. M. T*he DIRDIF-94 program system*, Technical Report for the Crystallography Laboratory; University of Nijmegen: The Netherlands, 1994.

(31) (a) Sheldrick, G. M. *SHELXS-97*, Programs for Solving X-ray Crystal Structures; University of Göttingen, 1997. (b) Sheldrick, G. M. *SHELXL-97*, Programs for Refining X-ray Crystal Structures; University of Göttingen, 1997.